

Coupled Nonlinear Oscillators

Roberto Sassi

1 Introduction

Mutual synchronization is a common phenomenon in biology. It occurs at different levels, ranging from the small scale of the cardiac pace-maker cells of the SA (Sino-Atrial) and AV (Atrium-Ventricular) nodes in the human hearth that synchronously fire and give the pace to the whole muscle, to the coordinated behaviours of crickets that chirp in unison and of fireflies that flash together in some parts of southeast Asia.

The dynamics of coupled oscillators is a very broad field of research; the approach we have chosen is only one of the many that are possible. The question we would like to answer is something like: “*What special phenomena can we expect to arise from the rhythmical interaction of whole populations of periodic processes?*” [1].

Winfree [1] was the first to underline the generality of the problem, fixing the first assumptions for a mathematical model. In his work each *oscillating species* (cell, or cricket, or firefly) is modeled as a nonlinear oscillator with a globally attracting limit cycle; The oscillators were assumed to be weakly coupled and their natural frequencies to be randomly distributed across the population.

Kuramoto [2] proposed the first model (called for this reason the *Kuramoto model*). His assumptions were that each oscillator is equal to the others, upto the frequency and phase, that the system has a *mean field* coupling and that the amplitudes of the oscillations are all the same (phase-only model). The equation of the model for the n oscillator is:

$$\frac{d\theta_n}{dt} = \omega_n + \frac{K}{N} \sum_{j=1}^N \sin(\theta_j - \theta_n) + \xi_n, \quad (1)$$

where K is the *coupling strength*, ω_n is a random variable with probability density function $g(\omega)$ and ξ_n is white noise.

Defining as *order parameter* the complex number,

$$r e^{i\psi} = \frac{\sum_{j=1}^N e^{i\theta_j}}{N}, \quad (2)$$

it's possible to *measure* the synchronization among the oscillators phases: $r = 0$ corresponds to the completely incoherent state, finite r to synchronization.

Kuramoto determined that $r = 0$ is always a steady solution; but there exists, in the case of no added random noise, a critical value of the coupling parameter $K_c = \frac{2}{\pi g(0)}$ below which only incoherent populations exist ($r = 0$). For $K > K_c$ a population of synchronized oscillators can exist ($r > 0$).

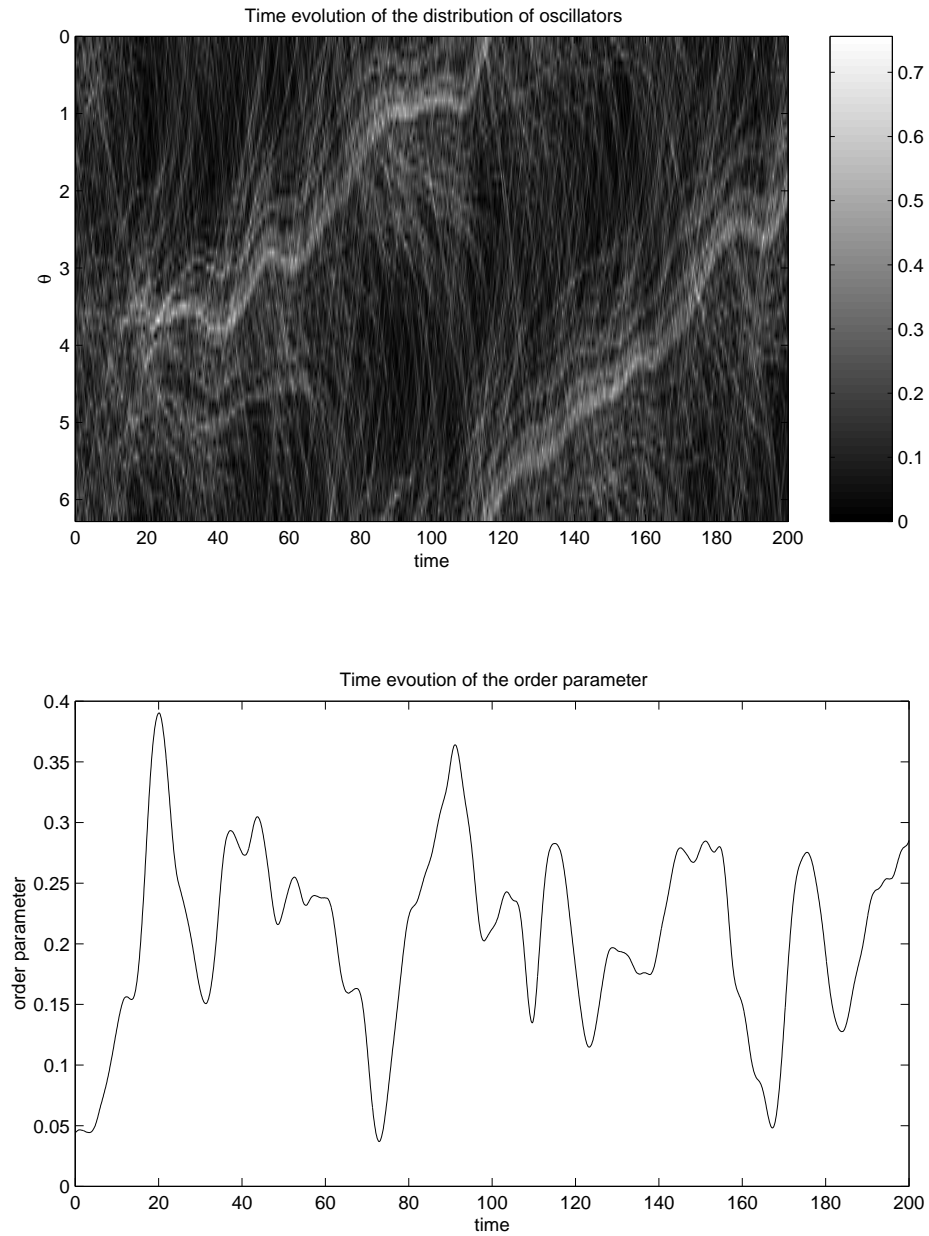


Figure 1: Numerical simulations on the discrete Kuramoto model with $N = 256$, $D = 0.01$, $K = 0.65$; (*upper*) time evolution of the probability density function computed on the trajectories of the system splitting up the θ axis in sub-intervals; (*lower*) time evolution of the absolute value of the order parameter

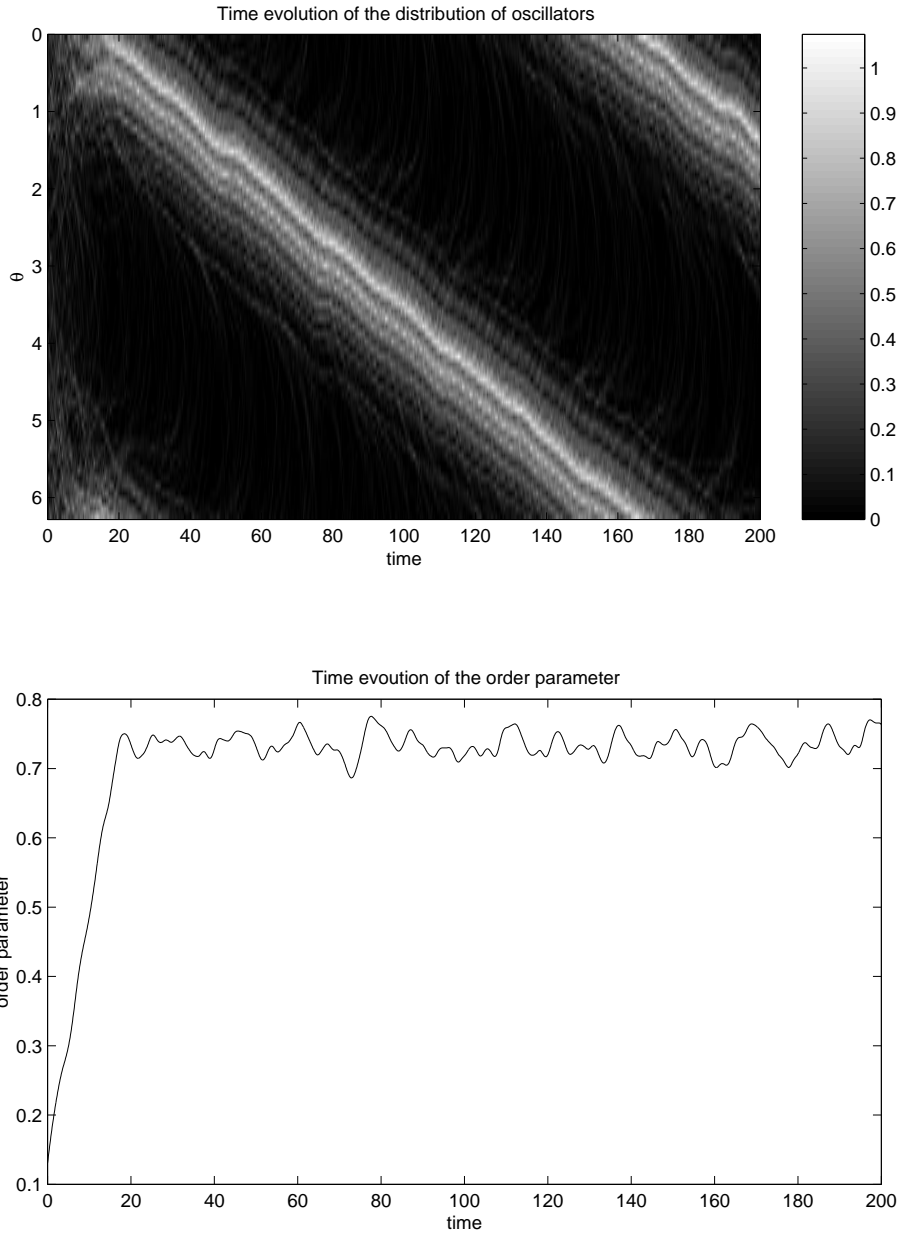


Figure 2: Numerical simulations on the discrete Kuramoto model with $N = 256$, $D = 0.01$, $K = 0.8$; (*upper*) time evolution of the probability density function computed on the trajectories of the system splitting up the θ axis in sub-intervals; (*lower*) time evolution of the absolute value of the order parameter

The results of the numerical simulations, performed solving equation (1) with $N = 256$ and two different values of the coupling parameter K , are shown in figures (1) and (2); in the upper panels the time evolution of the discrete probability density function ¹ is plotted; in the lower panels, the time evolution of the order parameter is displayed. The initial condition is, in both cases, a population of oscillators with phases uniformly distributed in $[0, 2\pi]$.

When $K = 0.8 > K_c$, in a very short time, the phases of the oscillators *gather* together in a small range of angles and then begin drifting coherently. The order parameter grows quickly and exhibits small oscillations due to the random noise added to the system (figure (2)).

A different situation arises with $K = 0.65 < K_c$; a coherent behaviour never starts, even if small structures can be noticed: small population of oscillators synchronize and drift for short periods of time. This is reflected in the order parameter that oscillates between 0 and 0.3 and decreases only slowly (figure (1)).

1.1 A continuous model

Using the approach sketched in the previous paragraph, it's difficult to go much farther; it's not easy, for example, to answer questions such as "*Is the coherent state ($K > K_c$) stable?*"

Strogatz & Mirollo [3] introduced a partial differential equation that describes the behaviour of the Kuramoto model in the limit $N \rightarrow \infty$.

The idea is that, in the continuous limit, the state is described by a probability density function: $\rho(\theta, \omega, t)$. The Kuramoto equation (1) becomes:

$$v = \omega + K \int_{-\infty}^{\infty} \int_0^{2\pi} \sin(\phi - \theta) \rho(\phi, \omega, t) g(\omega) d\phi d\omega, \quad (3)$$

where v is the *velocity* at the point (θ, ω, t) . Moreover, the density function ρ has to satisfy, for each given ω , a normalization law

$$\int_0^{2\pi} \rho d\theta = 1; \quad (4)$$

and a Fokker-Plank-type conservation law ²

$$\frac{\partial}{\partial t} \rho(\theta, \omega, t) + \frac{\partial}{\partial \theta} (\rho(\theta, \omega, t) v(\theta, \omega, t)) = D \frac{\partial^2}{\partial \theta^2} \rho(\theta, \omega, t), \quad (5)$$

¹The θ axis is divided into 64 intervals and, at each instant of time, the normalized histogram of the phases of the oscillators is computed.

²The derivation of the two equations has the flavor of the BBGKY hierarchy in plasma physics and can be found in [4]. Some rationalization of equation (5) can be given on recollecting that because the probability is conserved,

$$\begin{aligned} \frac{\partial}{\partial t} \int_{\theta_1}^{\theta_2} \rho(\theta) d\theta &= \rho(\theta_1) v(\theta_1) - \rho(\theta_2) v(\theta_2) \\ &= - \int_{\theta_1}^{\theta_2} \frac{\partial}{\partial \theta} (\rho v) d\theta \\ \rho_t &= - \frac{\partial}{\partial \theta} (\rho v), \end{aligned}$$

and on remembering Einstein's derivation of the diffusion equation in his work on the explanation of the

where $\theta \in [0; 2\pi]$ and $\omega \in [-\infty; \infty]$.

The *order parameter* (2), in the continuous limit, becomes:

$$re^{i\psi} = \int_{-\infty}^{\infty} \int_0^{2\pi} e^{i\theta} \rho(\theta, \omega, t) g(\omega) d\theta d\omega. \quad (6)$$

2 Linear Stability Theory

Strogatz & Mirollo [3] worked on the linear stability of the continuous Kuramoto equation. We will try to sketch the main results, useful for the discussion that follows.

With direct substitution into the equations (3) and (5), it can be seen that $\rho_0 = \frac{1}{2\pi}$ is a steady state solution for the system; it corresponds to the incoherent state with $r = 0$.

By linearizing ρ around the steady state solution, that is

$$\rho = \rho_0 + \epsilon(c(\omega, t)e^{i\theta} + c^*(\omega, t)e^{-i\theta}) + h.h.,$$

where ϵ is a small parameter and c^* is the complex conjugate of c , then substituting into (3) and introducing the notation

$$G(\omega, t) = \int_{-\infty}^{\infty} \int_0^{2\pi} \sin(\phi - \theta) \rho(\phi, \omega, t) g(\omega) d\phi d\omega,$$

it can be seen that G is different from zero only for functions that have a component on the bases $e^{i\theta}$ and $e^{-i\theta}$. That is, the higher harmonics do not give any contribution and the linearized equation (5) becomes

$$c_t = -(D + i\omega)c + \frac{K}{2} \int_{-\infty}^{\infty} c(\nu, t) g(\nu) d\nu. \quad (7)$$

The discrete spectrum can be computed by seeking solutions of the form $c(\omega, t) = b(\omega)e^{\lambda t}$. By substituting into equation (7), multiplying by $g(\omega)$ and integrating over ω , one finds the *dispersion relation*,

$$1 = \frac{K}{2} \int_{-\infty}^{\infty} \frac{g(\nu)}{\lambda + D + i\nu} d\nu. \quad (8)$$

When λ is negative, the order parameter decays and the system reverts to the incoherent state; *vice versa* for λ positive, the order parameter exponentially grows and this is, in the coupled oscillators system, the onset of synchronization.

The system has, also, a continuous spectrum at $\omega = -iD$ (see [3]). As the dissipation is always positive, the modes in the continuous spectrum are either all decaying or, at most, neutrally stable when $D = 0$.

Brownian motion [5], which indicates that

$$\begin{aligned} \rho_t &= 2\langle \xi^2 \rangle \rho_{\theta\theta} \\ &= D\rho_{\theta\theta} \end{aligned}$$

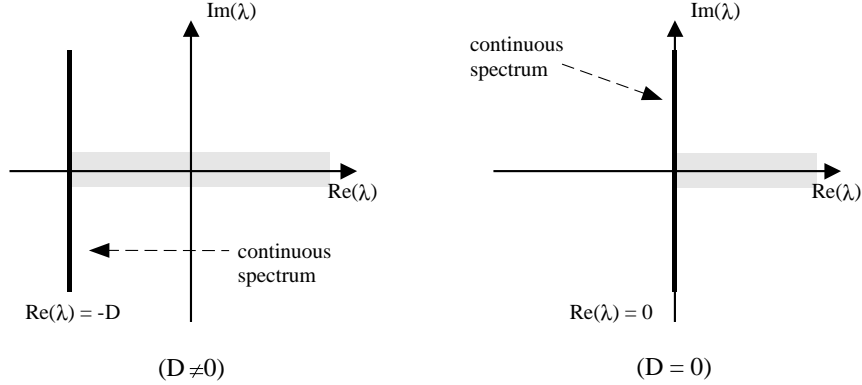


Figure 3: Continuous spectrum for the dispersion relation (8) either for the case $D \neq 0$ (left) and for the noise-free case with $D = 0$ (right). The discrete spectrum is composed of only one mode that exists for $K > K_c$ and lies to the right of the continuous spectrum (inside the *grey* region in the picture); in the noise-free case the discrete mode either is unstable or doesn't exist.

2.1 An example

Choosing as probability density function a lorentzian, that is

$$g(\omega) = \frac{1}{\pi} \frac{1}{\omega^2 + 1},$$

the *dispersion relation* can be solved analytically; the computed growing rate λ is

$$\text{sgn}(\lambda + D)\lambda = \frac{K}{2} - 1 + D$$

and the critical coupling (that is the value of K at which the system is neutrally stable) is

$$K_c = 2(1 + D).$$

If $D = 0$, then $K_c = \frac{2}{\pi g(0)}$; this is the same result that Kuramoto found working on the discrete system, as described in the introduction.

Summarizing, for $K \leq 2$, the system does not have any discrete mode; for $2 < K < K_c$ the system is stable and exponentially decaying; if $K = K_c$ it has a neutral mode and with $K > K_c$ an unstable growing mode (figure (3(left))).

It's interesting to notice that, if the dissipation is zero, the system can only be either unstable, with a growing mode ($K > K_c$), or neutrally stable, with no mode ($K \leq K_c$) (figure (3(right))). But, looking at figure (4(right)), it can be seen that the order parameter is, however, decaying exponentially.

How can we explained this apparent contradiction? Let's look at the solution of the initial value problem with $K < K_c$ and the initial condition

$$c(\omega, 0) = \frac{2}{\pi} \frac{1}{\omega^2 + 4}.$$

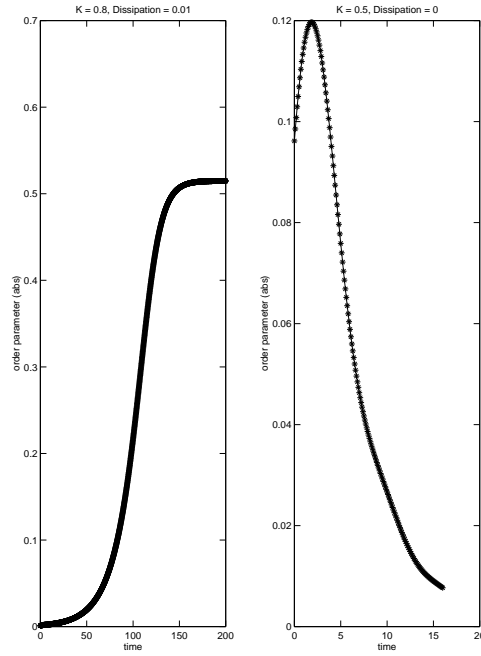


Figure 4: Time evolution of the order parameter for the Kuramoto continuous model; compact support within $[-1; 1]$ for $g(\omega) = \frac{1}{\pi-2} \frac{1-\omega^2}{1+\omega^2}$; initial condition $\tilde{\rho}_0 = \frac{1}{2\pi}$ and $\tilde{\rho}_1 = \xi \frac{2}{\pi} \frac{1}{4+\omega^2}$; (*left*) $D = 0.01$, $K_c = 0.739$, $\xi = 0.001$ and $K = 0.8$: over-critical coupling, the order parameter grows linearly and then, when the nonlinearity becomes strong enough, saturates; (*right*) $D = 0$, $K_c = 2 - \frac{4}{\pi}$, $\xi = 0.1$ and $K = 0.5$: under-critical coupling, the order parameter grows, initially, and then decays.

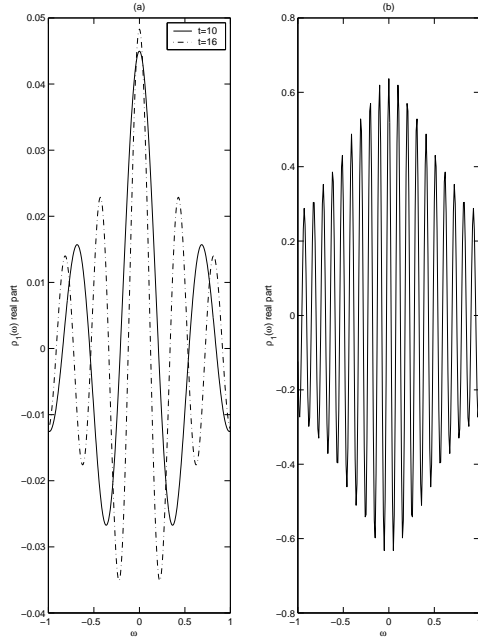


Figure 5: (a): real part of the first Fourier component of $\rho(\theta, \omega, t)$ at two different times, obtained with the numerical simulation described in figure 4(right). (b): real part of the first Fourier component of $\rho(\theta, \omega, t)$ at time $t = 60$ analytically computed. In both case is possible to observe the increasing number of oscillations.

Integrating equation (7) via Laplace's transform, we find that

$$c(\omega, t) = \left\{ \frac{2}{\pi} \frac{1}{\omega^2 + 4} - \frac{1}{3\pi} \frac{5}{2i\omega - 1} - \frac{1}{3\pi} \frac{1}{2 - i\omega} \right\} e^{i\omega t} + \frac{5}{3\pi} \frac{1}{2i\omega - 1} e^{-(\frac{\kappa}{2}-1)t} + \frac{1}{3\pi} \frac{1}{2 - i\omega} e^{-2t}.$$

Evidently, the function $c(\omega, t)$ is proportional to the non-decaying and non-separable term $e^{i\omega t}$. As time goes on, this term becomes increasingly crenellated.

What we are seeing here is equivalent to the Landau damping in plasma physics; the order parameter is proportional to the integral of the function $c(\omega, t)$; even if the latter doesn't decay, as soon as it starts crenellating, the positive and negative part cancel and the integral decreases.

In fact, computing the absolute value of the order parameter, we have

$$r = \frac{10}{3} e^{-(\frac{\kappa}{2}-1)t} - \frac{4}{3} e^{-2t}$$

which decays exponentially as $t \rightarrow \infty$.

3 Numerical Integration

The integration of the discrete model (equation (1)) has been performed with a fixed step ($\Delta t = 0.1$), fully-implicit predictor-corrector scheme. The fixed time step is forced by the

noise added to the derivatives that avoids the convergence of most adaptative methods.

In the continuous model (equations (5) and (3)) the density function ρ is periodic with period 2π , so the latter can be expanded in the Fourier series:

$$\rho(\theta, \omega, t) = \sum_{m=-\infty}^{\infty} \tilde{\rho}(\theta, t) e^{im\theta}$$

Substituting into the equations (5) and (3), we obtain the system of nonlinear ordinary differential equations for the Fourier coefficients $\tilde{\rho}_m$:

$$\begin{aligned} \tilde{\rho}_{0t} &= 0, \\ \tilde{\rho}_{mt} &= -K\pi m \langle \tilde{\rho}_{-1} \rangle \tilde{\rho}_{m+1} - (im\omega + Dm^2) \tilde{\rho}_m + K\pi m \langle \tilde{\rho}_1 \rangle \tilde{\rho}_{m-1} \\ &\text{for } m \neq 0 \end{aligned}$$

where

$$\langle f(\omega) \rangle = \int_{-\infty}^{\infty} f(\omega) g(\omega) d\omega \quad (9)$$

For each value of ω , truncating the Fourier series at $m = L$, the system can be efficiently integrated (a semi-implicit Adams-Bashfort-Moulton predictor-corrector scheme leads to the inversion of a tri-diagonal matrix). We used $L = 16, 32, 64, 128$ in the computations; the smaller the dissipation or the longer time windows considered, the bigger the number of Fourier components necessary to approximate properly the Kuramoto system. We found $L = 32$ a good compromise in many situations.

A little more attention is needed for the evaluation of the integral (9). We found that the most efficient way of computing it is via Gauss-Legendre quadrature formulae, setting compact support for $g(\omega)$, and using the solution for ρ , produced at the previous available time step.

In figures (6) and (7) the solutions computed for $\rho(\theta, \omega, t)$ are shown; in the sub-critical case, when the coupling parameter K is smaller than K_c , stripes of probability can be noticed, which increase in number and, slightly tilting, start shrinking. At fixed θ , this is the same crenellation as described above and seen in figure (5).

When $K > K_c$, in the super-critical case, the probability gathers, initially, in a stripe-like area, but immediately also starts to deplete from the central region. Unlike before, the number of stripes doesn't increase (in this case there's no Landau damping); two areas collect the whole probability. The process is reminiscent of the formation of a shock layer in the white regions in figure (7), but a truly weak solution does not form due to the dissipation introduced by the noise.

4 A symmetry property

Looking at the numerical results of the previous section, it can be observed that, starting from $\rho(\theta, \omega, 0)$ and $g(\omega)$ which are even functions in ω , a symmetry is preserved during the evolution of the dynamics; that is $\rho(\theta, \omega, t) = \rho(-\theta, -\omega, t)$. This behaviour can be explained in a general way.

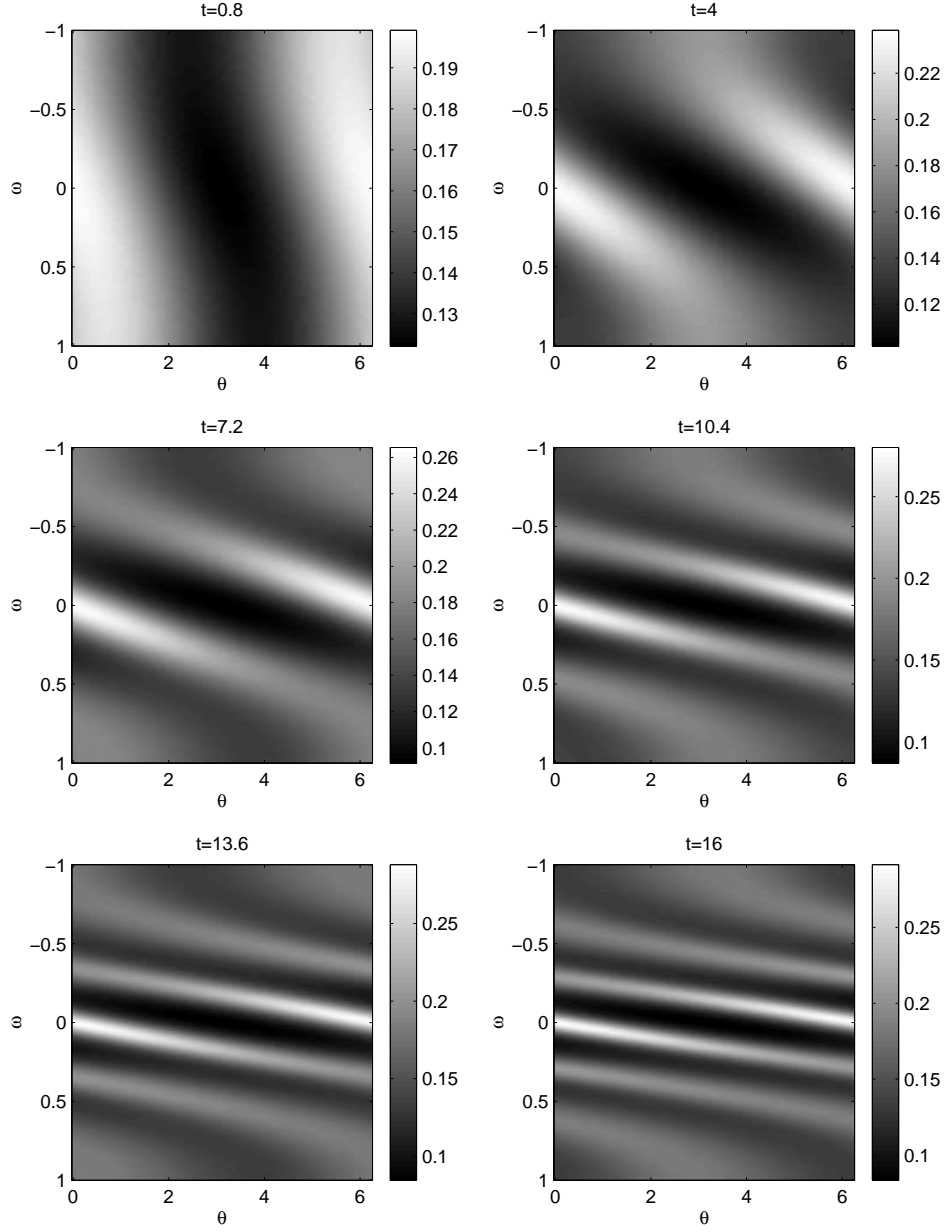


Figure 6: $\rho(\theta, \omega, t)$ at six successive instant of time obtained via numerical integration of the Kuramoto continuous model with $D = 0$ and $K = 0.5$ (see figure (4)(right) for further details). The coupling K is sub-critical.

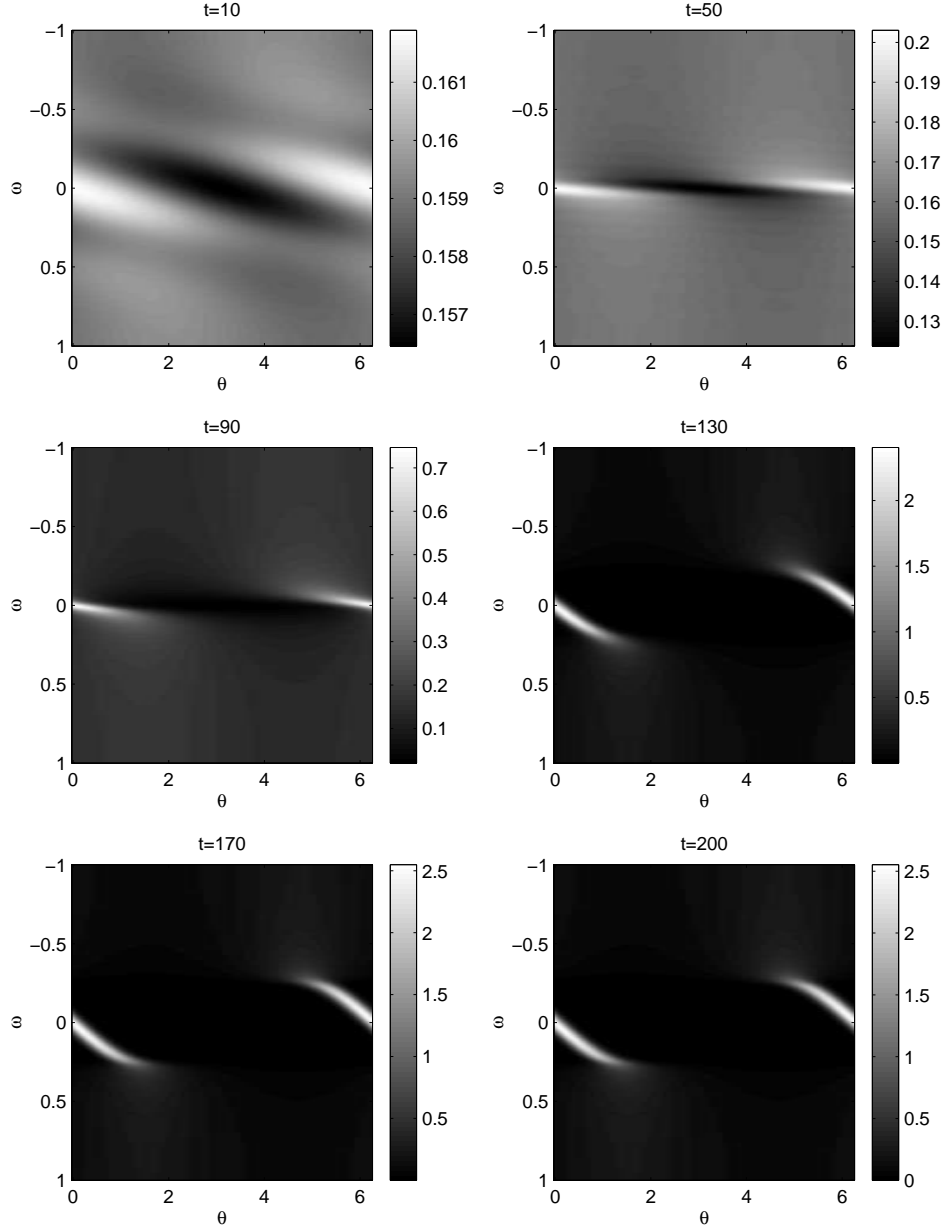


Figure 7: $\rho(\theta, \omega, t)$ at six successive instant of time obtained via numerical integration of the Kuramoto continuous model with $D = 0.01$ and $K = 0.8$ (see figure (4)(right) for further details). The coupling K is super-critical.

Let's start stating that the probability density function is so that, for each integer n ,

$$\rho(\theta, \omega, t) = \rho(\theta + 2\pi n, \omega, t) = \rho(2\pi n - \theta, -\omega, t) = \rho(-\theta, -\omega, t). \quad (10)$$

The symmetry property will be proved by construction.

Let's expand $\sin(\phi - \theta)$ in equation (3); the first integral can be rewritten

$$\begin{aligned} & \int_{-\infty}^{\infty} \int_{-\pi}^{\pi} \sin(\phi) \rho(\phi, \omega, t) g(\omega) d\phi d\omega \\ &= \int_{-\infty}^{\infty} \int_{-\pi}^0 \sin(\phi) \rho(\phi, \omega, t) g(\omega) d\phi d\omega + \\ & \quad \int_{-\infty}^{\infty} \int_0^{\pi} \sin(\phi) \rho(\phi, \omega, t) g(\omega) d\phi d\omega; \end{aligned} \quad (11)$$

If we make the change of variables $\phi' = -\phi$ and $\omega' = -\omega$ and we use equation (10), expression (11) becomes

$$\begin{aligned} (11) &= - \int_{-\infty}^{\infty} \int_0^{\pi} \sin(\phi') \rho(\phi', \omega', t) g(\omega') d\phi' d\omega' + \\ & \quad \int_{-\infty}^{\infty} \int_0^{\pi} \sin(\phi) \rho(\phi, \omega, t) g(\omega) d\phi d\omega \\ &= 0. \end{aligned}$$

At the end,

$$\begin{aligned} G(\theta, t) &= -\sin(\theta) \int_{-\infty}^{\infty} \int_{-\pi}^{\pi} \cos(\phi) \rho(\phi, \omega, t) g(\omega) d\phi d\omega \\ &= -\mathcal{G}(t) \sin(\theta). \end{aligned} \quad (12)$$

Substituting (12) into equation (5), it can be noticed that $\rho(-\theta, -\omega, t)$ is a solution of the Kuramoto model.

5 Weakly Nonlinear Theory

When $K = K_c$, the system is, by definition, linearly neutrally stable. In this situation and for $D \neq 0$, Bonilla & al. [6] and Crawford [7] developed an asymptotic expansion around the equilibrium solution and derived a Landau-type ordinary differential equation for the amplitude of the perturbation.

Defining $\epsilon \ll 1$, they chose the scalings,

$$\begin{aligned} \epsilon^2 t &= T \\ \partial_t &= \partial_T \epsilon^2, \end{aligned}$$

where T is the *slow time* (when t is very big, T is small),

$$K = K_c + \epsilon^2 K_2 + \dots$$

and expanded the function ρ such that

$$\begin{aligned}
\rho(\theta, \omega, T) &= \frac{1}{2\pi} + \\
&= \epsilon(\rho_1(\omega)a_1(T)e^{i\theta} + \rho_1^*(\omega)a_1^*(T)e^{-i\theta}) + \\
&= \epsilon^2(\rho_2(\omega)a_2(T)e^{i\theta} + \rho_2^*(\omega)a_2^*(T)e^{-i\theta}) + \\
&= \epsilon^3(\rho_3(\omega)a_3(T)e^{i\theta} + \rho_3^*(\omega)a_3^*(T)e^{-i\theta}) + \\
&= o(\epsilon^4).
\end{aligned}$$

From equations (5) and (3) it follows that

$$\epsilon^2 \frac{\partial \rho}{\partial T} = -\omega \frac{\partial \rho}{\partial \theta} - \frac{\partial}{\partial \theta} \rho K \int_{-\infty}^{\infty} \int_0^{2\pi} \sin(\phi - \theta) \rho g(\omega) d\phi d\omega + D \frac{\partial^2 \rho}{\partial \theta^2}$$

and

$$G = \epsilon G_1 + \epsilon^2 G_2 \dots$$

At the first order ($O(\epsilon)$) :

$$\rho_1 = \frac{K \int_{-\infty}^{\infty} \rho_1(\nu) g(\nu) d\nu}{2(\omega - iD)}.$$

Continuing to $O(\epsilon^3)$, eventually, one derives the amplitude equation,

$$a_{1T} = \frac{K_2}{2} a_1 + (K_c \pi)^2 \mathcal{I} |a_1|^2 a_1$$

where

$$\mathcal{I} = \int_{-\infty}^{\infty} \frac{\rho_1 g(\omega)}{\omega - 2iD} d\omega = \text{constant}$$

We can see from the expression for ρ_1 that this kind of approach is not satisfactory when $D = 0$; ρ diverges at $\omega = 0$, but as long as it's a probability density, this can not have any physical meaning and has to be avoided.

5.1 Weakly Nonlinear Theory: $D \neq 0$, but small

In this section we try to sketch how it's possible to develop an asymptotic expansion for the case $1 \gg D \neq 0$. Let's choose the variables to scale as in the previous case (Hopf scaling) but let's say that $D = \epsilon^2 D_2$. The motivation for this scaling can be found in the numerical experiments we performed and in the analysis by Daido and Crawford [4].

Substituting, as in the previous paragraph, into the equations (5) and (3) we have

$$\epsilon^2 \rho_T + \left(\frac{G_\theta}{2\pi} + (\rho G)_\theta \right) (K_c + \epsilon^2 K_2) = \epsilon^2 D_2 \rho_{\theta\theta}$$

and at the first and second order we can derive the following expressions for ρ_1 and ρ_2 :

$$\begin{aligned} O(\epsilon) &: \omega\rho_{1\theta} + \frac{G_{1\theta}K_c}{2\pi} = 0, \\ \rho_1 &= -\frac{K_c G_1}{2\pi\omega} \\ O(\epsilon^2) &: \omega\rho_{2\theta} + \frac{G_{2\theta}K_c}{2\pi} = -K_c(\rho_1 G_1)_\theta, \\ \rho_2 &= \frac{K_c^2 G_1^2}{2\pi\omega^2} - \frac{K_c G_2}{2\pi\omega}. \end{aligned}$$

Here is the problem we have to overcome; to treat properly the case $D \ll 1$ we need a critical layer around $\omega = 0$; in fact, at this point, the asymptotic expansion breaks down and ρ_2 is bigger than ρ_1 .

Inside the critical layer, we set the new independent and dependent variables

$$\begin{aligned} \omega &= \epsilon y \\ \rho &= Z(\theta, y, T) = Z_0 + \epsilon Z_1. \end{aligned}$$

The equation in the inner region becomes

$$\epsilon^2 Z_T + \epsilon y Z_\theta + \left(\frac{G_\theta}{2\pi} + (ZG)_\theta\right)(K_c + \epsilon^2 K_2) = \epsilon^2 D_2 Z_{\theta\theta}$$

and at the first two orders

$$\begin{aligned} O(\epsilon) &: yZ_{0\theta} + \frac{G_{1\theta}K_c}{2\pi} + K_c(Z_0 G_1)_\theta = 0, \\ Z_0 &= -\frac{1}{2\pi} \frac{K_c G_1}{y + K_c G_1} \\ O(\epsilon^2) &: yZ_{1\theta} + \frac{G_{2\theta}K_c}{2\pi} + (Z_1 G_1)_\theta K_c = \\ &-Z_{0T} - (Z_0 G_2)_\theta K_c + D_2 Z_{0\theta\theta}, \\ &((y + K_c G_1)Z_1 + \frac{K_c G_2}{2\pi})_\theta = \\ &\mathcal{F}\left(\frac{G_{1T}}{(y + K_c G_1)^2}, \frac{G_{1\theta}}{(y + K_c G_1)^2}, \frac{D_2 G_{1\theta}^2}{(y + K_c G_1)^3}\right) \end{aligned}$$

where \mathcal{F} is a function, that for our purpose we not need derive.

Even in the inner region we still have trouble: when $y + K_c G_1 = 0$, Z_0 diverges and Z_1 diverges even more; the asymptotic expansion breaks down another time.

This is very peculiar; the first inner layer is not sufficient at all and it's necessary for another critical layer, a second, inside the first. Moreover the shape of this inner layer is peculiar: it develops around the curve $y + K_c G_1 = 0$. The whole situation is sketched in figure (8).

In this second inner layer we define the new independent variable

$$y + K_c G_1 = \epsilon^\alpha \xi$$

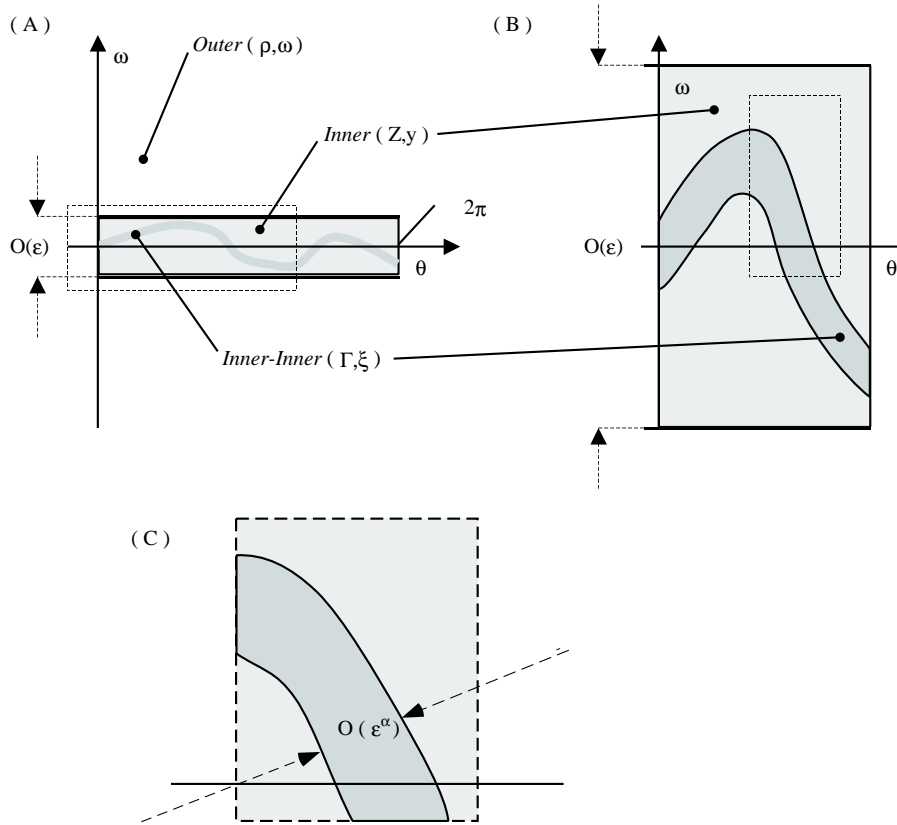


Figure 8: Weakly Nonlinear Theory. (A): When the dissipation is small ($O(\epsilon^2)$) a critical layer becomes necessary around the frequency $\omega = 0$ (*light gray region*); the width of this layer is of order ϵ . (B): The sketched-box in (A) is enlarged: inside is possible to notice the second “snake-like” critical layer (*inner-inner layer, dark gray region*), that is necessary around the line $y + K_c G_1 = 0$. (C): The sketched-box in (B) is enlarged again: the width of the inner-inner layer is of order ϵ^α ($\alpha = 1$ if $D_2 = 0$; $\alpha = 1/2$ if $D_2 \neq 0$).

and the new dependent variable

$$Z = \Gamma\left(\theta, \frac{y + K_c G_1}{\epsilon^\alpha}, T\right).$$

Deriving a new equation, in this second inner layer, is very technical and we will not develop it. The reason lies in the strange relation between T , θ and ξ , imposed by the shape of the layer. On the change of variable to ξ , the θ and T derivatives pick up additional ξ -derivatives,

$$\begin{aligned} [Z_\theta]_{y,T} &= [\Gamma_\theta]_{\xi,T} + \frac{K_c G_\theta}{\epsilon^\alpha} [\Gamma_\xi]_{\theta,T} \\ [Z_T]_{y,\theta} &= [\Gamma_T]_{\xi,\theta} + \frac{K_c G_\theta}{\epsilon^\alpha} [\Gamma_\xi]_{T,\theta} \end{aligned}$$

and this makes it much more complex to derive useful analytical expressions.

We conclude this section sketching an argument for determining the scaling parameter α . We can deduce from the relations (13) the scaling for Z_0 and Z_1 ,

$$\begin{aligned} O(\epsilon) &: Z_0 \sim O(\epsilon^{-\alpha}) \\ O(\epsilon^2) &: Z_1 \sim O(\epsilon^{-2\alpha}) \quad OR \quad D_2 \epsilon^{-3\alpha}. \end{aligned}$$

Hence Z_1 scales in different way depending on the value of D_2 .

We now apply the condition that Z_0 and ϵZ_1 have to scale at the same order, which is where the expansion formally breaks down and we enter the innermost region. There are two different situations, depending upon the value of D_2 : if $D_2 = 0$, then $\alpha = 1$, and when $D_2 \neq 0$, then $\alpha = 1/2$. The reason of the scaling we chose for D becomes, now, more clear and we would have lost this double behaviour with a higher scaling of the noise term ($D \rightarrow \epsilon^\beta D$ with $\beta > 2$).

Summarizing the results in this section, when D is finite but small, the derived asymptotic expansion reveals that we need, at least, two critical layers, one inside the other. The first, around $\omega = 0$, is of order ϵ ; the second, snake-shaped, is inside the first and has a characteristic width that depends upon the value of D_2 .

6 Steadily propagating solutions

In this section we look for steadily propagating solutions for ρ , that is

$$\rho(\theta, \omega, t) = \rho(\theta - \Omega t, \omega),$$

where Ω is the propagation velocity.

Substituting this expression into equation (3) and making the change of variable $\Phi = \phi - \Omega t$, we find

$$\begin{aligned} G(\theta, t) &= \int_{-\infty}^{\infty} \int_0^{2\pi} \sin(\phi - \theta) \rho(\phi - \Omega t, \omega) g(\omega) d\phi d\omega \\ &= \int_{-\infty}^{\infty} \int_0^{2\pi} \sin(\Phi - (\theta - \Omega t)) \rho(\Phi, \omega) g(\omega) d\Phi d\omega \\ &= G(\theta - \Omega t, \omega). \end{aligned}$$

From this, we can observe that G preserves the dependence on $(\theta - \Omega t)$ that ρ is supposed to have.

Equation (5), in the situation $D = 0$, becomes

$$(\omega - \Omega)\rho_\theta + k(G\rho)_\theta = 0; \quad (13)$$

integrating over θ

$$\rho = \frac{\mathcal{J}(\omega)}{\omega - \Omega + kG(\theta - \Omega t)} \quad (14)$$

where $\mathcal{J}(\omega)$ is a generic function of ω .

As N.J.B. says in these situations, *we are in bad shape*; as long as ρ is a probability distribution function, it can not have singularity; as long as ω is a real variable that spans the entire real axis, the pole from the denominator of ρ is hard to avoid.

This is an interesting point; if the dissipation is zero the system does not admit steadily propagating solutions. But what happens when the dissipation is *small*?

If $D \neq 0$, equation (13) has an additional term, and after the integration over θ , we have

$$(\omega - \Omega)\rho + kG\rho = \mathcal{J}(\omega) + D\rho_\theta. \quad (15)$$

For the sake of simplicity, let's say that we have *fixed* ω to a certain value; then there's a value of $\Theta = \theta - \Omega t$ at which the denominator of equation (14) vanishes; we call this value Δ .

As $D \rightarrow 0$, ρ scales as $1/(\Theta - \Delta)$; hence we need an inner layer in the proximity of $\Theta - \Delta = 0$ in which the dissipative term becomes important. For this reason we choose the following scaling and variables,

$$\begin{aligned} \Theta - \Delta &= \epsilon\delta \\ \rho &= \frac{1}{\epsilon}R \\ D &= \epsilon^2 \end{aligned}$$

Substituting in equation (15) and noting that $\partial_\theta = \partial_\Theta = \epsilon^{-2}\partial_\delta$ we have

$$kG_\Theta(\Delta)\delta R = \mathcal{J}(\omega) + R_\delta$$

Integrating over δ , we can find the expression of the probability distribution function in the inner layer and check the condition for the matching with the outer:

$$\begin{aligned} R_\delta &= kG_\Theta(\Delta)\delta R - \mathcal{J}(\omega) \\ (Re^{\frac{-kG_\Theta(\Delta)\delta^2}{2}})_\delta &= -\mathcal{J}(\omega)e^{\frac{-kG_\Theta(\Delta)\delta^2}{2}} \\ R &= R_0e^{\frac{kG_\Theta(\Delta)\delta^2}{2}} - \mathcal{J}(\omega)e^{\frac{kG_\Theta(\Delta)\delta^2}{2}} \int_{-\infty}^{\delta} e^{\frac{-kG_\Theta(\Delta)\bar{\delta}^2}{2}} d\bar{\delta}. \end{aligned}$$

The value of R_0 can be computed with the normalization condition (4).

This solution is potentially dangerous; it has to be bounded, otherwise it again diverges; moreover in the limit of δ going to infinity (that is, going *out* of the inner layer) R has still

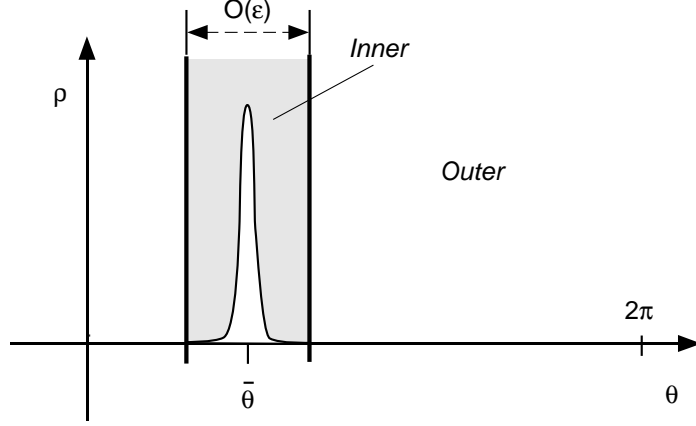


Figure 9: Steadily propagating solution with $\Omega = 0$: a sketch of $\rho(\theta, \omega)$. Near the phase $\bar{\theta}$ (where $\omega + KG(\bar{\theta}) = 0$ and $G'(\bar{\theta}) < 0$) a critical layer (*light gray region*) is necessary. In the outer layer ρ is zero everywhere.

to be limited, for a proper matching with ρ . Using these two conditions, we fix the value of $\mathcal{J}(\omega)$ and R_0

$$\begin{aligned} \mathcal{J}(\omega) &= 0 \quad \text{for } G_{\Theta}(\Delta) < 0, \\ \mathcal{J}(\omega) &= 0, R_0 = 0 \quad \text{for } G_{\Theta}(\Delta) > 0, \end{aligned} \quad (16)$$

The matching with the outer layer is straightforward; as δ goes to infinity, R it's zero and ρ is zero everywhere. In figure (9) is shown a sketch of the situation for $\Omega = 0$.

Summarizing this result, steadily propagating solution can not develop for $D = 0$; with D finite, but small, they exist only in a small layer, that follows the line $(\omega - \Omega + kG(\theta - \Omega t)) = 0$ where $G_{\Theta}(\Delta) < 0$.

The probability density ρ is exponentially small everywhere in the outer layer; for this reason the integral for G is limited to the inner, and

$$\begin{aligned} G(\Theta, t) &= \int_{-\infty}^{\infty} \int_0^{2\pi} \sin(\Phi - \Theta, t) \rho(\Phi, \omega) g(\omega) d\Phi d\omega \\ &= \int_{-\infty}^{\infty} \int_{-\infty}^{\infty} \sin(\Delta(\omega) - \Theta, t) R_0 e^{\frac{kG_{\Theta}(\Delta)\delta^2}{2}} g(\omega) d\delta d\omega \end{aligned}$$

6.1 An example: $\Omega = 0$

Let's say that $\Omega = 0$, so that we look for a steady solution of the kind $\rho(\theta, \omega)$. In this case, steadily propagating solutions can develop only along the line $\omega + KG(\theta) = 0$.

Choosing a symmetric initial condition and applying relation (12), the curve becomes

$$\omega = KG(t) \sin(\theta).$$

Moreover, along the line, solutions can form only where $G_\theta < 0$, that is

$$\begin{aligned} -\mathcal{G}(t) \frac{d \sin(\theta)}{d\theta} &< 0 \\ \frac{d \sin(\theta)}{d\theta} &> 0, \end{aligned}$$

as K and \mathcal{G} are both positive. In figure (10) this *prediction* is compared to the actual solution, obtained with the numerical simulations. As it can be seen, the agreement is evident and this explains the depletion of probability noticed in the middle of the plane θ - ω , in figure (7).

7 The case $g(\omega) = \delta(\omega)$

In the previous two sections we appreciate that, if we set D small, but different from zero, it's possible to perform an asymptotic expansion and steadily propagating solutions can develop. But what happens when $D = 0$? The described approach only underlined that this is a critical situation. In this section, with $D = 0$, we will show how is possible to solve analytically the Kuramoto equations in the case that $g(\omega)$ is a Dirac's delta function.

In this case all the oscillators share the same frequency $\omega = 0$ and have different phases. Starting from a symmetric initial condition, that is $\rho(\theta, 0) = \rho(-\theta, 0)$, and using property (12), equations (5) and (3) become

$$\begin{aligned} \rho_t(\theta, 0, t) - k \partial_\theta (\rho(\theta, 0, t) \sin(\theta)) \int_0^{2\pi} \int_{-\infty}^{\infty} \cos(\phi) \rho(\phi, 0, t) \delta(\omega) d\omega d\phi &= 0 \\ \rho_t(\theta, t) - k \partial_\theta (\rho(\theta, t) \sin(\theta)) \int_0^{2\pi} \cos(\phi) \rho(\phi, t) d\phi &= 0; \end{aligned}$$

Setting

$$\mathcal{F}(t) = \int_0^{2\pi} \cos(\phi) \rho(\phi, t) d\phi,$$

the last relation becomes

$$\rho_t - k \sin(\theta) \mathcal{F}(t) \rho_\theta = k \cos(\theta) \mathcal{F}(t) \rho. \quad (17)$$

We solve this equation by the method of characteristics; for equation (17) the characteristic equation is

$$\frac{dt}{1} = \frac{d\theta}{-k \sin(\theta) \mathcal{F}(t)} = \frac{d\rho}{k \cos(\theta) \mathcal{F}(t) \rho}.$$

Hence,

$$\begin{aligned} \frac{d\theta}{dt} &= -k \sin(\theta) \mathcal{F}(t) \\ \frac{d\rho}{dt} &= k \cos(\theta) \mathcal{F}(t) \rho. \end{aligned}$$

Solving the first, we obtain

$$\tan\left(\frac{\theta}{2}\right) = \tan\left(\frac{\theta_0}{2}\right) e^{-k \int_0^t \mathcal{F}(t') dt'}; \quad (18)$$

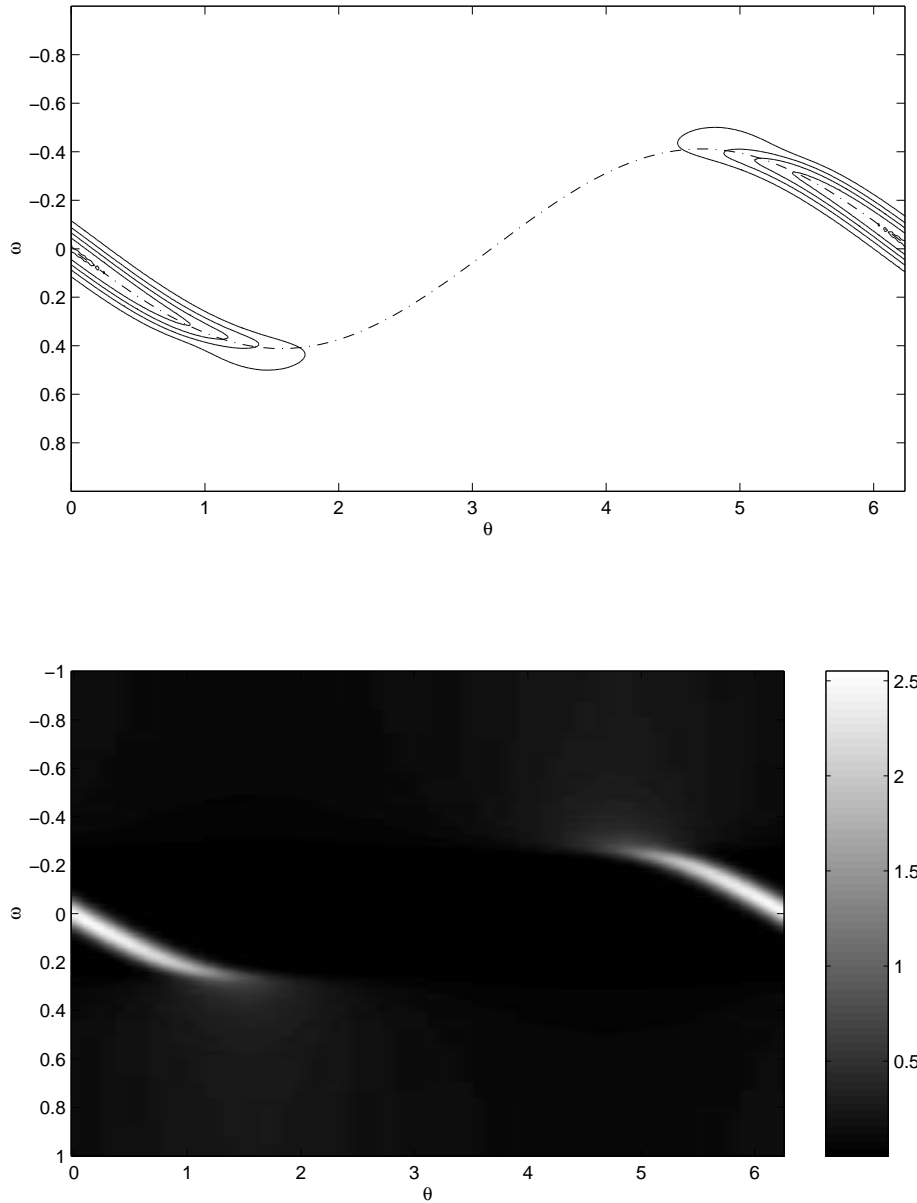


Figure 10: $\rho(\theta, \omega, t)$ at $t = 180$ obtained via numerical integration of the Kuramoto continuous model with $D = 0.01$ and $K = 0.8$ (see figure (4)(left) for further details). *UPPER*: contour plot of ρ ; the super-imposed sketched line is $\omega = K\mathcal{G}(t) \sin(\theta)$. The steadily propagating solution (with $\Omega = 0$) can develop only where $G'(\theta) < 0$, as expected. *LOWER*: plot of ρ . Looking back to figure (7) is now possible to understand why the probability is zero in the middle of the pictures.

dividing the first with the second

$$\begin{aligned}\frac{d\rho}{d\theta} &= -\rho \cot(\theta) \\ \rho \sin(\theta) &= \text{constant} = \rho_0(\theta_0(\theta, t)) \sin(\theta_0(\theta, t)).\end{aligned}$$

The derivation here becomes a little *technical*:

$$\begin{aligned}\rho &= \rho_0 \frac{\frac{2 \tan(\theta_0/2)}{1+\tan^2(\theta_0/2)}}{2 \sin(\theta/2) \cos(\theta/2)} = \rho_0 \frac{\frac{2 \tan(\theta/2)\mathcal{E}(t)}{1+\tan^2(\theta/2)\mathcal{E}^2(t)}}{2 \sin(\theta/2) \cos(\theta/2)} \\ &= \rho_0 \frac{e^{-kq}}{e^{-2kq} \cos^2(\theta/2) + \sin^2(\theta/2)}\end{aligned}$$

where $q = \int_0^t \mathcal{F}(t') dt'$ and $\mathcal{E} = e^{kq}$.

As time goes on, we expect the order parameter to saturate to a certain constant value; this is what we saw in the numerical simulations. The order parameter is, by definition, proportional to G by a factor 2π . Calling $\overline{\mathcal{F}}$ the saturation value of G then q , the integral of \mathcal{F} , becomes

$$q \sim \overline{\mathcal{F}}t \quad \text{as } t \rightarrow \infty.$$

Choosing, now, the initial condition $\rho_0 = \cos(\theta_0)$, and recalling relation (18), we find

$$\begin{aligned}\rho_0 &= \frac{1 - \tan^2(\theta_0/2)}{1 + \tan^2(\theta_0/2)} = \frac{1 - \tan^2(\theta/2)\mathcal{E}^2}{1 + \tan^2(\theta/2)\mathcal{E}^2} \\ &= \frac{e^{-2kq} \cos^2(\theta/2) - \sin^2(\theta/2)}{e^{-2kq} \cos^2(\theta/2) + \sin^2(\theta/2)}\end{aligned}$$

Finally, substituting ρ_0 into the expressions for ρ and q we have

$$\rho = e^{-kq} \frac{e^{-2kq} \cos^2(\theta/2) - \sin^2(\theta/2)}{(e^{-2kq} \cos^2(\theta/2) + \sin^2(\theta/2))^2}$$

and

$$\frac{dq}{dt} = e^{-kq} \int_0^{2\pi} \cos(\theta) \frac{e^{-2kq} \cos^2(\theta/2) - \sin^2(\theta/2)}{(e^{-2kq} \cos^2(\theta/2) + \sin^2(\theta/2))^2} d\theta \quad (19)$$

The integral in (19) can be evaluated in the limit that q goes to infinity. Making the change of variable $\theta = 2xe^{-kq}$ and expanding in Taylor's series the trigonometric functions, it becomes:

$$\begin{aligned}\frac{dq}{dt} &= \int_{-\infty}^{\infty} \frac{-2x^2}{(1+x^2)^2} dx = -2\pi \\ q &= -2\pi t\end{aligned}$$

Summarizing, as the time goes on, q grows linearly; ρ becomes small everywhere except near $\theta = 0$ where $\rho \sim e^{kq}$, so that it grows exponentially. The dynamics brings probability

toward a singular phase (the point $\theta = 0$ here); this is exactly what we saw in the numerical simulation, although with different $g(\omega)$, and along a curve on the (θ, ω) plane.

Concluding, the solution is a spike-shaped shock-like object. This is also consistent with another fact, which is namely that, with $g(\omega) = \delta(\omega)$ and the alternative coupling, $\sin(\phi - \theta) \rightarrow \delta(\phi - \theta)$, the Kuramoto model reduces to the Burger's equation,

$$\rho_t(\theta, 0, t) + [K\rho^2(\theta, 0, t)]_\theta.$$

8 Discrete vs. Continuous

An important question is whether the continuous approximation, made in the limit $N \rightarrow \infty$, remains valid with a relatively small number of oscillators. That is, if the results, obtained in the previous sections, are applicable to equation (1).

We don't have a final answer to such a question, but, comparing figures (11) and (12), obtained from the discrete model with $N = 256$, with (6) and (7), can be seen that the main behaviours are the same. In particular, in figure (12), we see the probability gathering in two symmetric areas of the plane, as in the continuous case of figure (7).

A peculiarity of the discrete case is that the concentration of probability drifts in the θ direction; we suppose this to be related to the fact that, although the probability density function, from which the initial condition is extracted, is symmetric, the actual initial condition is not.

9 Conclusions and other remarks

The Kuramoto model generates many interesting results; many more than what we were expecting. So, in this report, for brevity reasons, we have omitted several of the analyses we made. We mention two particular ones here:

First, we studied the issue of transient amplification: starting from a situation of equilibrium with a sub-critical coupling, and imposing perturbations of different intensities, one can find solutions to the linear initial-value problem that grow to arbitrarily large amplitude before decaying. One important question is whether this transient growth induces nonlinear behaviour in the full system before the disturbance can decay. But, from the numerical simulations, the system appears to be very robust, with a decay that is very much similar to what predicted by the linear theory no matter how big the transient growth. In other words, the nonlinearity of the system doesn't provide any new, unexpected behaviours.

Second, we also applied Nyquist methods to the linear stability problem: in the linear analysis section we computed analytically the value of the growth rate and the critical value of the coupling parameter for the Lorentzian. For general $g(\omega)$, the integral in (8) can be solved numerically to furnish similar results, but in many situations it is helpful to have a quick, general understanding. We used the Nyquist criteria to derive the following result that, here, we only state: *the maximum number of unstable growing rates, for the linearized Kuramoto system, is the number of monotonic pieces of $g(\omega)$ divided by two.*

On the other hand, there is further work to be done in at least two different directions:

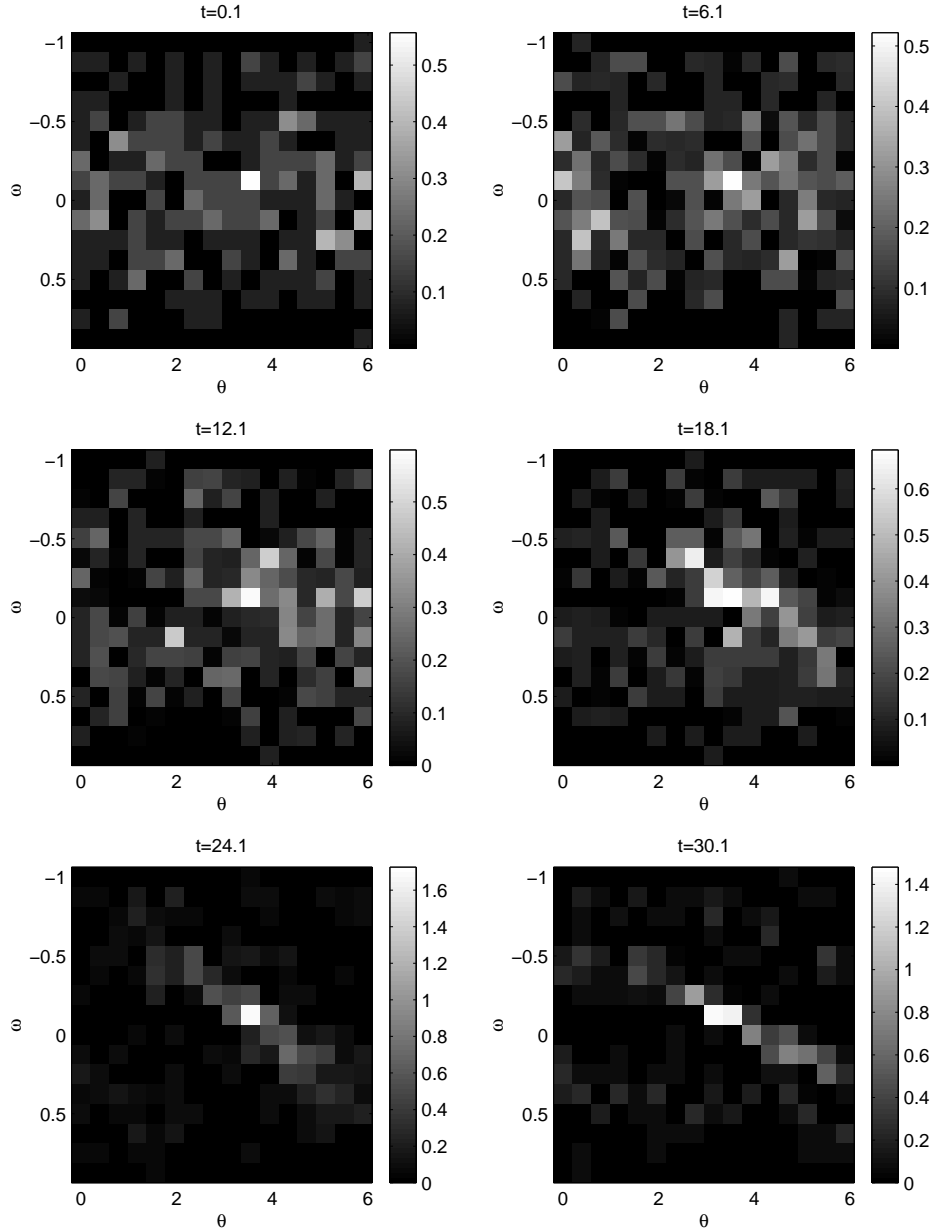


Figure 11: $\rho(\theta, \omega, t)$ at six successive instant of time obtained via numerical integration of the Kuramoto discrete model with $D = 0.01$ and $K = 0.65$ ($K_c = 0.739$, *sub-critical coupling*). Both θ and ω axes are discretized in 16 intervals. Compact support within $[-1; 1]$ for $g(\omega) = \frac{1}{\pi-2} \frac{1-\omega^2}{1+\omega^2}$; initial condition $\tilde{\rho}_0 = \frac{1}{2\pi}$ and $\tilde{\rho}_1 = \xi \frac{2}{\pi} \frac{1}{4+\omega^2}$ with $\xi = 0.1$.

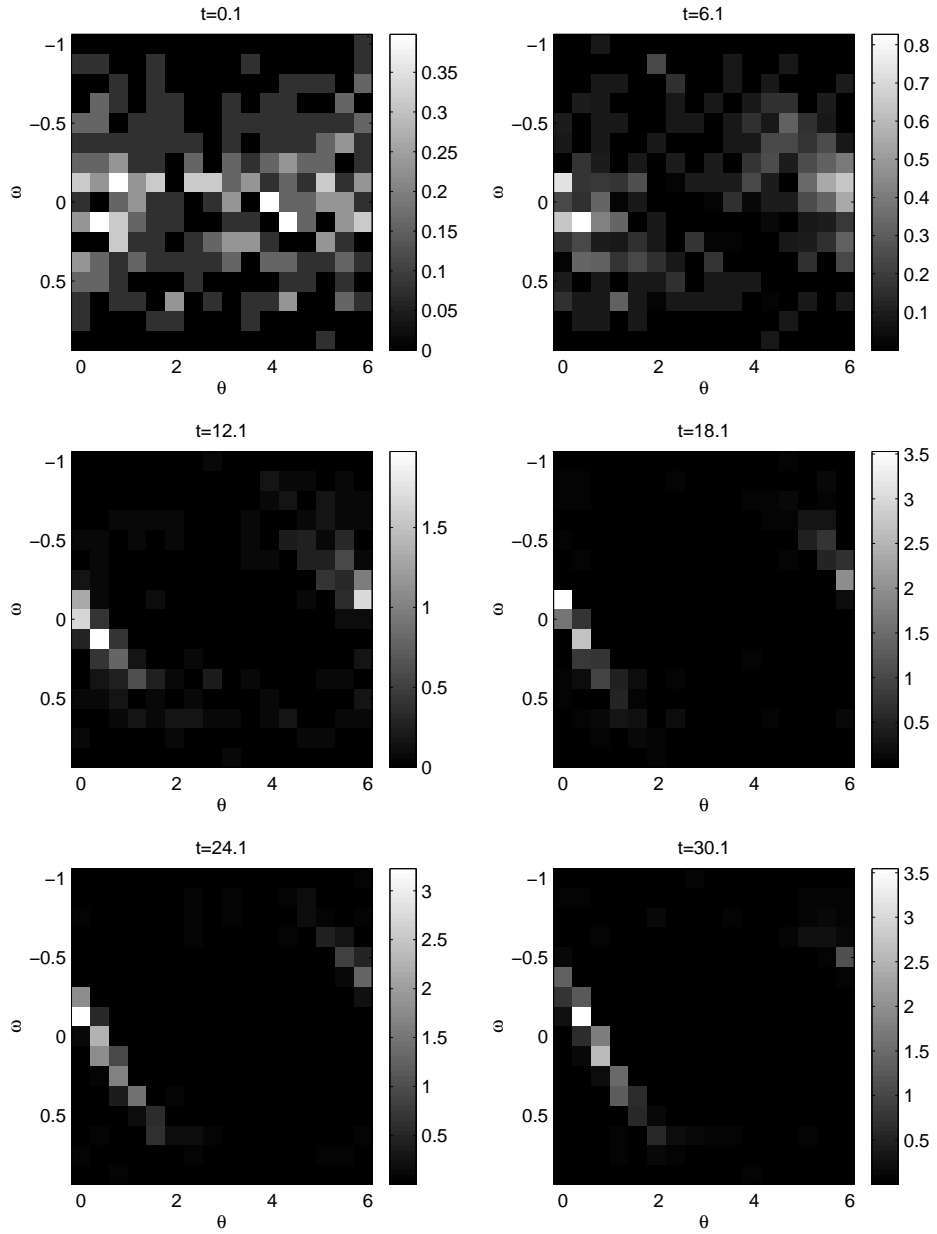


Figure 12: The same as in figure (11) except $K = 0.8$ (*super-critical coupling*).

- the comparison of the discrete and continuous model is only sketched and needs more numerical explorations. Moreover, do traveling solutions, as we saw in figure (12), exist in the continuous case? In figure (1) structures can be noticed, even if the coupling is sub-critical and we are expecting incoherence. What is the origin of these structures? Do they only depend on the initial condition?
- The change in the form of the coupling seems to be critical (see ad example [4] and [8]). What happen if the coupling is different than $\sin(\phi - \theta)$? Why?

10 Acknowledgments

The first person I like to thank is Neil J. Balmforth that suggested this work and followed me on each step, all the summer long. Then I'm grateful to Francesco Paparella that helped me with the numerical computations; to W. R. Young, Rick Salmon, Phil Morrison, Jean-Luc Thiffeault and Stefan G. Llewellyn Smith for aid and very useful conversations.

In particular thank to Ed Spiegel, that first suggested me to come to Woods Hole this summer and that helped me several times with his car.

The work I did this summer would have been impossible without the help of the other fellows. Apart from that, we lived almost together for ten weeks so there are thousands of reasons to say thank for. Among them I like to say thank to Claudia Pasquero that cooked for everyone so many times; to Yuan-Nan Young that shared with me a very small room in the Barn; to Pascale Garaud that, restless, organized a lot of nice after-dinner events; to David Osmond that introduced the fellows to the *triathlon* and showed me how to repair the bike; to Jennifer *Jen* MacKinnon for having explained me the difference between walnuts and pecans; to Raffaele Ferrari for listening me so many times about my non-working code; to Jennifer *Niffer* Curtis that made me *DrPepper's freak*; to Jeffrey *Jeff* Moehlis and his wife Allison for the *GFD cooler*; to Meredith Metzger for her internet radio; and again to Jean-Luc Thiffeault for being Canadian.

At the end, I like to thank George Veronis that taught *how to play softball* to the fellows and that was happy though we lost all the games we played; moreover he had his sailboat repaired so that I tried sailing, for the first time, on the pond in front of his cottage.

References

- [1] A. T. Winfree, "Biological rhythms and the behavior of populations of coupled oscillators," *J. Theoret. Biol.* **16**, 15 (1967).
- [2] Y. Kuramoto, in *International symposium on mathematical problems in theoretical physics*, No. 39 in *Lecture Notes in Physics*, edited by H. Araki (Springer, New York, 1975), pp. 420–422.
- [3] S. H. Strogatz and R. E. Mirollo, "Stability of incoherence of a population of coupled oscillators," *J. Stat. Phys.* **63**, 613 (1991).

- [4] J. D. Crawford and K. T. R. Davies, “Synchronization of globally coupled phase oscillators: singularities and scaling for general couplings,” *Phys. D* **125**, 1 (1999).
- [5] A. Einstein, *Investigations on the Theory of the Brownian Movement* (Dover Publications, New York, 1985).
- [6] L. L. Bonilla, J. C. Neu, and R. Spigler, “Nonlinear stability of incoherence and collective synchronization in a population of coupled oscillators,” *J. Stat. Phys.* **67**, 313 (1992).
- [7] J. D. Crawford, “Amplitude expansions for instabilities in populations of globally-coupled oscillators,” *J. Stat. Phys.* **74**, 1047 (1994).
- [8] L. L. Bonilla, C. J. P. Vicente, and R. Spigler, “Time-periodic phases in populations of nonlinearly coupled oscillators with bimodal frequency distributions,” *Phys. D* **113**, 79 (1998).